JACS
JOURNAL OF THE AMERICAN CHEMICAL SOCIETY

Communication

pubs.acs.org/JACS

Hexathienocoronenes: Synthesis and Self-Organization

Long Chen,[†] Sreenivasa R. Puniredd,[†] Yuan-Zhi Tan,[†] Martin Baumgarten,[†] Ute Zschieschang,[‡] Volker Enkelmann,[†] Wojciech Pisula,[†] Xinliang Feng,[†] Hagen Klauk,[‡] and Klaus Müllen*[,†]

[†]Max Planck Institute for Polymer Research, Ackermannweg 10, 55128 Mainz, Germany

[‡]Max Planck Institute for Solid State Research, Heisenbergstr. 1, 70569 Stuttgart, Germany

Supporting Information

ABSTRACT: Here we report hexathienocoronenes (HTCs), fully thiophene-annelated coronenes in which six double bonds in the periphery are thieno-fused. The derivatives tetrasubstituted with hexyl and dodecyl chains show a phase formation that strongly depends on the chain length. HTCs are remarkably stronger donors than the known thiophene-annelated coronenes but do not readily assemble into well-ordered films when deposited from the vapor phase. Thus, thin-film transistors fabricated by vacuum deposition have only modest field-effect mobilities of 0.002 $cm^2\ V^{-1}\ s^{-1}$.

Polycyclic aromatic hydrocarbons (PAHs) can be regarded as two-dimensional graphene segments. Because of their optoelectronic and self-assembling properties,[1] PAHs have served as active components of organic electronic devices such as field-effect transistors, light-emitting diodes, and solar cells.[2] Compared with their all-hydrocarbon analogues, PAHs containing heteroatoms such as N,[3] S,[4] or O[5a] in the aromatic skeleton, either neutral or positively charged,[5] exhibit unprecedented chemical and physical properties. Increasing attention has been paid to heterocyclic PAHs, especially those containing thiophene units.[6] To date, multiple-thiophene-fused benzene,[7] naphthalene,[8] anthracene,[9,18] triphenylene,[10] pyrene,[4d] tetracene,[11a−e] pentacene,[11f] and coronene[12] have been developed. We are particularly interested in thiophene-annelated coronenes for their interesting assembly behavior. Nuckolls[12a] described a contorted dibenzotetrathienocoronene (*c*-DBTTC), a tetrathiophene-fused version of the previously reported contorted hexabenzocoronene[13] (*c*-HBC), although *c*-DBTTC is flatter than its analogue *c*-HBC. Spurred by the beautiful structure of the first fully heterocyclic circulene, "sulflower" (octathio[8]-circulene),[4a] which has eight S atoms pointing out of the molecular plane, here we report hexathienocoronenes (HTCs), fully thiophene-annelated coronenes wherein six double bonds in the periphery are thieno-fused. The HTCs were obtained as inseparable mixtures of syn and anti isomers derived from the regioisomers of the anthradithiophene quinone precursor. To investigate the effect of the regioisomerism on the molecular packing and physical properties, a syn form, HTC *syn*-**1b**, was synthesized. The organization was studied by X-ray scattering of thin films. For two derivatives with hexyl and dodecyl substituents, the order and phase formation strongly depend on the length of the alkyl side chains.

The synthesis of the HTCs is shown in Scheme 1. The key building block is 5,11-bis(dibromomethylene)anthradithiophene (**4**). The conventional Corey−Fuchs (CF) reaction of anthradithiophene-5,11-dione (**3**) with PPh_3 and CBr_4 either in dichloromethane with stirring at room temperature[14] or refluxing in toluene[15] failed or gave only trace amounts of product because of the low reactivity of **3**. However, with a slightly modified procedure using $(i\text{-PrO})_3P$[16] instead of PPh_3, the CF reaction of **3** smoothly afforded **4** in 67% yield. Subsequently, fourfold Suzuki cross-coupling of **4** with thiophene-α-boronic esters **5** afforded the bisolefin skeletons **6** in high yields (86−89%). In contrast to Nuckolls' case, photocyclization of trimethylsilyl (TMS)-substituted **6b** gave only the half-closed product **7**,[17] while nonsubstituted **6a** afforded the nonsubstituted, fully cyclodehydrogenated HTC **2a** in 88% yield. On the other hand, **7** could be further dehydrogenated[17] using ferric chloride to obtain **2b**. For comparison, a TMS-substituted tetrathieno-[*a*,*c*,*j*,*l*]coronene (TMS-TTC) was also synthesized [Scheme S1 in the Supporting Information (SI)]. Toward a facile and efficient synthesis of HTCs, we used Suzuki coupling of thiophene-β-boronic ester **8** with **4** followed by photocyclization to afford the target HTCs **1** directly in high yields (65−92%). To investigate the effect of the regioisomerism on the molecular packing and physical properties, we also synthesized the

Scheme 1. Synthesis of HTCs 1 and 2 Based on 3

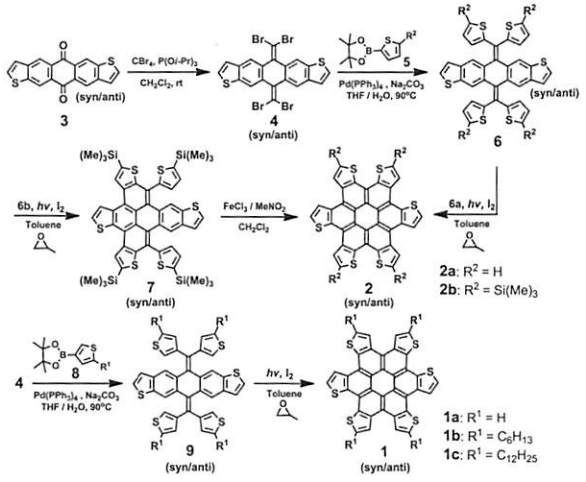

Received: August 20, 2012
Published: October 15, 2012

   dx.doi.org/10.1021/ja3082395 | *J. Am. Chem. Soc.* 2012, 134, 17869−17872

isomerically pure HTC *syn*-**1b** using *syn*-**3**[18] as the precursor (Scheme S2).

HTCs **1** and **2** were fully characterized by NMR spectroscopy, MALDI-TOF mass spectrometry, UV/vis absorption spectroscopy. MALDI-TOF mass spectra of **1** and **2** revealed single species with isotopic distributions in accordance with calculations (Figure S1 in the SI). UV/vis spectra of **2b** (Figure 1)

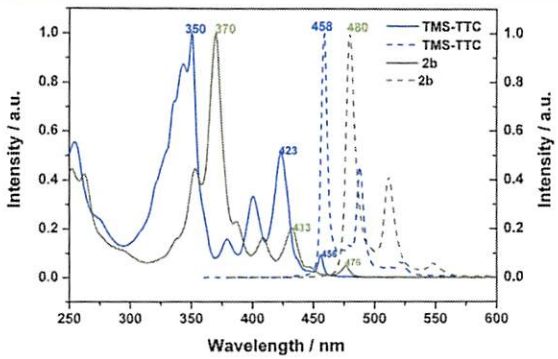

Figure 1. Normalized UV/vis spectra (solid) and photoluminescence (PL) spectra (dashed) of TMS-TTC (blue) and **2b** (green) (1.0×10^{-6} M in CH_2Cl_2). Three distinct emission bands with maxima at 458, 488, and 522 nm and at 480, 512, and 548 nm were observed in the PL spectra of **TMS-TTC** and **2b**, respectively.

showed three well-resolved absorption bands (α, β, p) characteristic of large PAHs. The absorption maximum of **2b** (β band, 370 nm, $\varepsilon = 2.48 \times 10^5$ M^{-1} cm^{-1}) exhibited a significant bathochromic shift (20 nm) relative to the corresponding band of TMS-TTC (350 nm, $\varepsilon = 1.83 \times 10^5$ M^{-1} cm^{-1}). The same bathochromic shift was observed for the α band of **2b** (476 nm) relative TMS-TTC (456 nm). However, a small bathochromic shift (10 nm) was found for the p band of **2b** (433 nm) relative to TMS-TTC (423 nm). **1** and **2** showed almost identical absorption bands, although the four thiophenes are annelated at different positions (Figure S2a). The absorption spectra of spin-coated films exhibited bathochromic shifts of 16 nm for both **1b** and **1c** and spectral broadening, indicating that the HTCs have a strong tendency to aggregate in the solid state (Figure S2b).

To elucidate the influence of the peripheral thiophenes on the molecular energy levels of the coronene core, the HOMO energies of the HTCs were obtained via cyclic voltammetry (Figure S3). For example, **2b** showed four quasi-reversible oxidation waves, with the onset of the first oxidation indicating a HOMO energy of −5.08 eV, which is in good agreement with calculations (−4.93 eV; Figure S4) and comparable to the values reported for [*a*,*g*,*m*]TTC (−5.51 eV)[12c] and *c*-DBTTC (−5.10 eV).[12a] The HOMO energies of **1b** and **1c** are −5.00 and −4.97 eV, respectively (Table S1 in the SI). Thus, the new HTCs are stronger donors than [*a*,*g*,*m*]TTC and *c*-DBTTC and might serve as efficient active layers in photovoltaic devices.[19]

The bulk thermotropic properties of HTCs **1b** and **1c** were investigated by differential scanning calorimetry (DSC) and polarized optical microscopy (POM). **1b** and **1c** showed only one main phase transition during cooling, related to their solidification from the isotropic melt. The transition temperatures were 232 °C for **1b** and 128 °C for **1c**, indicating the effect of the alkyl side chains on the thermal properties, as observed previously for other discotic PAHs[26](Figure S5). An additional peak at 38 °C for **1c** was assigned to reorganization of the substituent alkyl chains. The phase was further characterized by means of POM on thin films cooled from the isotropic phase. Slow cooling at 0.1 °C/min resulted in a highly birefringent fanlike texture (Figure 2a), as observed for discotic liquid-

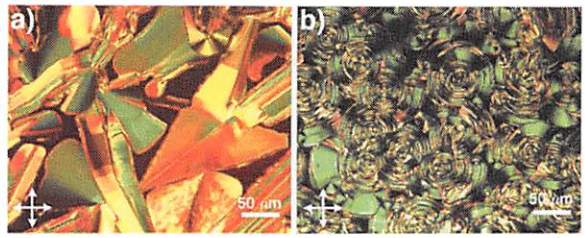

Figure 2. POM images of **1c** at cooling rates of (a) 0.1 and (b) 1 °C/min.

crystalline (LC) phases.[20] With more rapid thermal processing (1 °C/min), the shape of the texture changed to spiral, indicating that the columns were approximately parallel to the glass slides and that the molecules were tilted with respect to the column axis (Figure 2b).[21] This is in agreement with the structural analysis discussed below.

To provide a better understanding of the nature of the HTC molecules and their intermolecular interactions, single crystals of **1b** were grown from *p*-xylene solutions by slow evaporation at room temperature. Although these HTC materials existed as inseparable mixtures of syn and anti isomers, this did not significantly interfere with the packing in the crystal,[11f] as shown in Figure 3.[22a] In contrast to *c*-DBTTC, because of the relatively

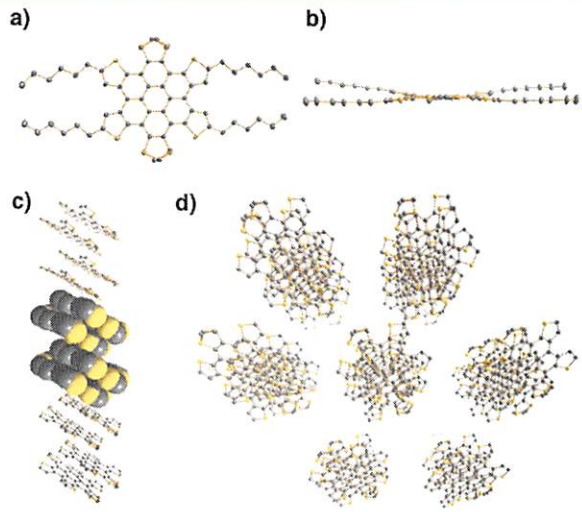

Figure 3. Crystal structure of **1b** obtained from *p*-xylene. (a) Top and (b) side views shown as ORTEP plots. (c) Side view of columnar packing with interlayer distances of 3.37 Å in the dimer stack and 3.5 Å between the dimers. (d) Eclipsed interlayer packing in the distorted hexagonal columnar arrangement. H atoms and the hexyl side chains in (c) and (d) have been removed for clarity. C, gray; S, yellow.

weak steric congestion of the six outer thiophene rings, **1b** adopts an almost planar conformation (Figure 3a,b); the maximal deviation of the C and S atoms from the molecular plane is 0.56 Å, and the angle between the plane of the outer thiophene and inner benzenoid rings is 7.4°. X-ray diffraction (XRD) also revealed the assembly of **1b**. Columnar packing was observed, with stacks of molecules oriented along the *a* axis. Interestingly, the repeating moiety with the stack is not the monomer; instead,

dx.doi.org/10.1021/ja3082395 | J. Am. Chem. Soc. 2012, 134, 17869–17872

dimers are packed in a graphite-like AB fashion (Figure 3c). Within the dimer stacks, the $\pi-\pi$ interactions dominate, with a distance of 3.37 Å between two molecules, while the distance between the dimers is expanded to ca. 3.5 Å. These molecular stacks are arranged in a distorted hexagonal arrangement of columns in the solid state (Figure 3d). Serendipitously, another crystal polymorph of **1b** was obtained from dilute toluene solution.[22b] Interestingly, this crystal polymorph of **1b** forms dimers by $\pi-\pi$ interactions with an expanded interlayer distance of 3.5 Å, with no obvious $\pi-\pi$ stacking among the dimers. Furthermore, the aromatic plane of **1b** is much more twisted (Figure S6). On the other hand, single crystals of isomerically pure *syn*-**1b** were also obtained by slow evaporation from *p*-xylene.[22c] However, the crystal structure of *syn*-**1b** was remarkably similar to that of the syn/anti mixture and also displayed disorder at two sulfur positions, probably because the molecules were simply flipped over in the lattice and present in equal abundance (Figure S7).[27] Comparison of the ^{13}C NMR spectra of *syn*-**9b** and *syn/anti*-**9b** together with the ^{1}H NMR spectrum of *syn*-**1b** showed much better resolution of peaks than for *syn/anti*-**1b**, further confirming that the observed disorder was not a result of the presence of a mixture of syn and anti isomers but appeared because half of the molecules were inverted in the crystal lattice (Figure S8).

To gain further insight into the supramolecular organization of **1b** and **1c** on the surface, grazing-incidence wide-angle X-ray scattering (GIWAXS) measurements on thin films were performed. The samples were prepared by drop-casting from toluene solution (2 mg/mL) with subsequent annealing at 90 °C. The GIWAXS pattern of **1b** indicates a crystalline phase with molecules arranged edge-on, while the columnar stacks are parallel to the surface (Figure 4a). An identical organization was

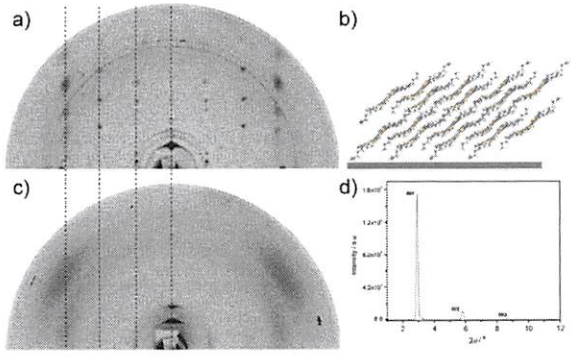

Figure 4. (a) GIWAXS pattern of a thin film of **1b** and (b) corresponding schematic illustration of the molecular organization on the surface. (c) GIWAXS pattern and (d) XRD of a thin film of **1c**. Dashed lines are guides for the reflections positioned on scattering lines.

recently determined for columnar terrylene diimides.[23] Meridional reflections along q_z for $q_{x,y}$ = 0 are related to an intercolumnar out-of-plane spacing of 1.84 nm. Further scattering lines parallel to q_z suggest a complex intracolumnar packing of the molecules. To clarify the surface organization, the single-crystal data for both solvents (toluene and *p*-xylene) were used to simulate the scattering patterns with Cerius^2 for comparison to the experimental results. As expected, only the simulated pattern for the crystal from toluene was in good agreement with the GIWAXS pattern (Figure S9). In this way, it was possible to derive precisely the molecular packing of **1b** on the surface after thermal treatment. The molecules are arranged with the alkyl chains pointing toward the substrate, and the aromatic cores are tilted ca. 45° toward the surface (Figure 4b). This correlates with the calculated molecular size of 2.58 nm [arccos(1.84/2.58) ≈ 45°]. On the basis of these findings, the GIWAXS pattern of **1c** was then analyzed (Figure 4c). The reflections related to the intracolumnar arrangement for **1c** are significantly broader than those for **1b** but are located on identical scattering lines at identical positions. This indicates not only a lower crystallinity for **1c** because of the longer flexible alkyl side chains but also a similar molecular organization on the surface. This latter conclusion was drawn from the first scattering line in the middle-angle region and the wide-angle off-meridional reflections, all of which were located at the same scattering angles as for **1b**. The out-of-plane spacing of 3.0 nm determined from the XRD plot (Figure 4d) is in agreement with the meridional plane of the GIWAXS pattern and is attributed to molecules tilted by ~45° [arccos(3.0/4.2) ≈ 45°]. The decreased order is related to the LC phase observed by POM.

Bearing in mind these highly ordered structures formed in the assemblies, we further investigated the charge transport properties in polycrystalline vacuum-deposited thin films of HTCs. **1a** and **1b** were selected for the first attempt because of their high crystallinity. Bottom-gate, top-contact thin-film transistors (TFTs) with a 110 nm thick SiO_2/AlO_x gate dielectric functionalized with a fluoroalkylphosphonic acid self-assembled monolayer[24] and a 30 nm thick vacuum-deposited semiconductor layer were fabricated. **1a** and **1b** were deposited at substrate temperatures of 100 and 120 °C, respectively. Figure S10 shows the output and transfer characteristics of the TFTs, which exhibited p-type behavior with field-effect mobilities of 0.002 $cm^2\ V^{-1}\ s^{-1}$ for **1a** and 0.001 $cm^2\ V^{-1}\ s^{-1}$ for **1b**. These mobilities are notably smaller than the best mobilities reported for TFTs based on oligoacenes[25] and thienoacenes.[6c,11] The reasons for these relatively small mobilities are the self-assembly into one-dimensional columnar stacks and the poor crystallinity of the vacuum-deposited thin films, as revealed by atomic force microscopy (Figure S11a,c) and XRD (Figure S11b,d). The poor crystallinity of the vacuum-deposited films is in stark contrast to the excellent crystallinity of the drop-cast films (see Figure 4), which suggests that solution processing may be a more suitable deposition method for HTCs.

In summary, we have reported unprecedented sulfur-containing heterocyclic PAHs and established a facile synthetic method for these fully thiophene-annelated coronenes that allows various substituents to be introduced easily. They reveal remarkable self-assembly behavior in solution, the solid state, and at the solution–substrate interface. HTC **1c** forms a columnar mesophase over a wide temperature range close to room temperature, which is much lower than that for the well-investigated hexadodecylhexabenzocoronene,[26] and thus is good for processing in electronic devices. Moreover, compared with the reported *c*-DBTTCs, the tetrasubstituted HTCs leave the two α-positions of the annelated thiophenes on the anthradithiophene backbone open, allowing further functionalization and polymerization.[27] Investigations of the formation of charge transfer complexes with acceptor counterparts (e.g., TCNQ) and polymerization of HTCs are currently underway.

■ ASSOCIATED CONTENT

Supporting Information

Synthetic details and characterization data. This material is available free of charge via the Internet at http://pubs.acs.org.

AUTHOR INFORMATION

Corresponding Author

muellen@mpip-mainz.mpg.de

Notes

The authors declare no competing financial interest.

ACKNOWLEDGMENTS

We thank the DFG Priority Program (SPP 1355, SPP1459) and ERC NANOGRAPH for support. L.C. is grateful for funding by the Alexander von Humboldt Foundation.

REFERENCES

(1) Hoeben, F. J. M.; Jonkheijm, P.; Meijer, E. W.; Schenning, A. P. H. J. *Chem. Rev.* **2005**, *105*, 1491.

(2) (a) Katz, H. E.; Bao, Z.; Gilat, S. L. *Acc. Chem. Res.* **2001**, *34*, 359. (b) Bendikov, M.; Wudl, F.; Perepichka, D. F. *Chem. Rev.* **2004**, *104*, 4891. (c) Schmidt-Mende, L.; Fechtenkötter, A.; Müllen, K.; Moons, E.; Friend, R. H.; MacKenzie, J. D. *Science* **2001**, *293*, 1119.

(3) (a) Matena, M.; Stöhr, M.; Riehm, T.; Björk, J.; Martens, S.; Dyer, M. S.; Persson, M.; Lobo-Checa, J.; Müller, K.; Enache, M.; Wadepohl, H.; Zegenhagen, J.; Jung, T. A.; Gade, L. H. *Chem.—Eur. J.* **2010**, *16*, 2079. (b) Draper, S. M.; Gregg, D. J.; Madathil, R. *J. Am. Chem. Soc.* **2002**, *124*, 3486. (c) Takase, M.; Enkelmann, V.; Sebastiani, D.; Baumgarten, M.; Müllen, K. *Angew. Chem., Int. Ed.* **2007**, *46*, 5524. (d) Bunz, U. H. F. *Chem.—Eur. J.* **2009**, *15*, 6780.

(4) (a) Chernichenko, K. Y.; Sumerin, V. V.; Shpanchenko, R. V.; Balenkova, E. S.; Nenajdenko, V. G. *Angew. Chem., Int. Ed.* **2006**, *45*, 7367. (b) Sun, Y.; Tan, L.; Jiang, S.; Qian, H.; Wang, Z.; Yan, D.; Di, C.; Wang, Y.; Wu, W.; Yu, G.; Yan, S.; Wang, C.; Hu, W.; Liu, Y.; Zhu, D. *J. Am. Chem. Soc.* **2007**, *129*, 1882. (c) Jiang, W.; Zhou, Y.; Geng, H.; Jiang, S.; Yan, S.; Hu, W.; Wang, Z.; Shuai, Z.; Pei, J. *J. Am. Chem. Soc.* **2010**, *133*, 1. (d) Zöphel, L.; Enkelmann, V.; Rieger, R.; Müllen, K. *Org. Lett.* **2011**, *13*, 4506.

(5) (a) Wu, D.; Pisula, W.; Haberecht, M. C.; Feng, X.; Müllen, K. *Org. Lett.* **2009**, *11*, 5686. (b) Wu, D.; Zhi, L.; Bodwell, G. J.; Cui, G.; Tsao, N.; Müllen, K. *Angew. Chem., Int. Ed.* **2007**, *46*, 5417.

(6) (a) Takimiya, K.; Ebata, H.; Sakamoto, K.; Izawa, T.; Otsubo, T.; Kunugi, Y. *J. Am. Chem. Soc.* **2006**, *128*, 12604. (b) Yamamoto, T.; Takimiya, K. *J. Am. Chem. Soc.* **2007**, *129*, 2224. (c) Shinamura, S.; Osaka, I.; Miyazaki, E.; Nakao, A.; Yamagishi, M.; Takeya, J.; Takimiya, K. *J. Am. Chem. Soc.* **2011**, *133*, 5024. (d) Niimi, K.; Shinamura, S.; Osaka, I.; Miyazaki, E.; Takimiya, K. *J. Am. Chem. Soc.* **2011**, *133*, 8732. (e) Zschieschang, U.; Kang, M. J.; Takimiya, K.; Sekitani, T.; Someya, T.; Canzler, T. W.; Werner, A.; Blochwitz-Nimoth, J.; Klauk, H. *J. Mater. Chem.* **2012**, *22*, 4273.

(7) (a) Nicolas, Y.; Blanchard, P.; Levillain, E.; Allain, M.; Mercier, N.; Roncali, J. *Org. Lett.* **2004**, *6*, 273. (b) Kashiki, T.; Shinamura, S.; Kohara, M.; Miyazaki, E.; Takimiya, K.; Ikeda, M.; Kuwabara, H. *Org. Lett.* **2009**, *11*, 2473. (c) Nielsen, C. B.; Fraser, J. M.; Schroeder, B. C.; Du, J.; White, A. J. P.; Zhang, W.; McCulloch, I. *Org. Lett.* **2011**, *13*, 2414.

(8) (a) Osaka, I.; Abe, T.; Shinamura, S.; Miyazaki, E.; Takimiya, K. *J. Am. Chem. Soc.* **2010**, *132*, 5000. (b) Shinamura, S.; Osaka, I.; Miyazaki, E.; Nakao, A.; Yamagishi, M.; Takeya, J.; Takimiya, K. *J. Am. Chem. Soc.* **2011**, *133*, 5024. (c) Osaka, I.; Abe, T.; Shinamura, S.; Takimiya, K. *J. Am. Chem. Soc.* **2011**, *133*, 6852. (d) Loser, S.; Bruns, C. J.; Miyauchi, H.; Ortiz, R. P.; Facchetti, A.; Stupp, S. I.; Marks, T. J. *J. Am. Chem. Soc.* **2011**, *133*, 8142. (e) Sanjaykumar, S. R.; Badgujar, S.; Song, C. E.; Shin, W. S.; Moon, S.-J.; Kang, I.-N.; Lee, J.; Cho, S.; Lee, S. K.; Lee, J.-C. *Macromolecules* **2012**, *45*, 6938. (f) Loser, S.; Miyauchi, H.; Hennek, J. W.; Smith, J.; Huang, C.; Facchetti, A.; Marks, T. J. *Chem. Commun.* **2012**, *48*, 8511.

(9) (a) Laquindanum, J. G.; Katz, H. E.; Lovinger, A. J. *J. Am. Chem. Soc.* **1998**, *120*, 664. (b) Payne, M. M.; Parkin, S. R.; Anthony, J. E.; Kuo, C.-C.; Jackson, T. N. *J. Am. Chem. Soc.* **2005**, *127*, 4986. (c) Mamada, M.; Minamiki, T.; Katagiri, H.; Tokito, S. *Org. Lett.* **2012**, *14*, 4062. (d) Nakano, M.; Niimi, K.; Miyazaki, E.; Osaka, I.; Takimiya, K. *J. Org. Chem.* **2012**, *77*, 8099.

(10) Endou, M.; Ie, Y.; Aso, Y. *Heterocycles* **2008**, *76*, 1043.

(11) (a) Tang, M. L.; Okamoto, T.; Bao, Z. *J. Am. Chem. Soc.* **2006**, *128*, 16002. (b) Yuan, Q.; Mannsfeld, S. C. B.; Tang, M. L.; Toney, M. F.; Lüning, J.; Bao, Z. *J. Am. Chem. Soc.* **2008**, *130*, 3502. (c) Tang, M. L.; Reichardt, A. D.; Miyaki, N.; Stoltenberg, R. M.; Bao, Z. *J. Am. Chem. Soc.* **2008**, *130*, 6064. (d) Tang, M. L.; Mannsfeld, S. C. B.; Sun, Y.-S.; Becerril, H. A.; Bao, Z. *J. Am. Chem. Soc.* **2009**, *131*, 882. (e) Tang, M. L.; Reichardt, A. D.; Wei, P.; Bao, Z. *J. Am. Chem. Soc.* **2009**, *131*, 5264. (f) Payne, M. M.; Odom, S. A.; Parkin, S. R.; Anthony, J. E. *Org. Lett.* **2004**, *6*, 3325.

(12) (a) Chiu, C.-Y.; Kim, B.; Gorodetsky, A. A.; Sattler, W.; Wei, S.; Sattler, A.; Steigerwald, M.; Nuckolls, C. *Chem. Sci.* **2011**, *2*, 1480. (b) Gorodetsky, A. A.; Chiu, C.-Y.; Schiros, T.; Palma, M.; Cox, M.; Jia, Z.; Sattler, W.; Kymissis, I.; Steigerwald, M.; Nuckolls, C. *Angew. Chem., Int. Ed.* **2010**, *49*, 7909. (c) Li, Z.; Zhi, L.; Lucas, N. T.; Wang, Z. *Tetrahedron* **2009**, *65*, 3417.

(13) (a) Xiao, S.; Myers, M.; Miao, Q.; Sanaur, S.; Pang, K.; Steigerwald, M. L.; Nuckolls, C. *Angew. Chem., Int. Ed.* **2005**, *44*, 7390. (b) Xiao, S.; Tang, J.; Beetz, T.; Guo, X.; Tremblay, N.; Siegrist, T.; Zhu, Y.; Steigerwald, M.; Nuckolls, C. *J. Am. Chem. Soc.* **2006**, *128*, 10700. (c) Guo, X.; Xiao, S.; Myers, M.; Miao, Q.; Steigerwald, M. L.; Nuckolls, C. *Proc. Natl. Acad. Sci. U.S.A.* **2009**, *106*, 691. (d) Plunkett, K. N.; Godula, K.; Nuckolls, C.; Tremblay, N.; Whalley, A. C.; Xiao, S. *Org. Lett.* **2009**, *11*, 2225.

(14) Hwang, G. T.; Son, H. S.; Ku, J. K.; Kim, B. H. *J. Am. Chem. Soc.* **2003**, *125*, 11241.

(15) Donovan, P. M.; Scott, L. T. *J. Am. Chem. Soc.* **2004**, *126*, 3108.

(16) Fang, Y.-Q.; Lifchits, O.; Lautens, M. *Synlett* **2008**, 413.

(17) Zhang, X.; Jiang, X.; Zhang, K.; Mao, L.; Luo, J.; Chi, C.; Chan, H. S. O.; Wu, J. *J. Org. Chem.* **2010**, *75*, 8069.

(18) (a) Lehnherr, D.; Hallani, R.; McDonald, R.; Anthony, J. E.; Tykwinski, R. R. *Org. Lett.* **2012**, *14*, 62. (b) Lehnherr, D.; Waterloo, A. R.; Goetz, K. P.; Payne, M. M.; Hampel, F.; Anthony, J. E.; Jurchescu, O. D.; Tykwinski, R. R. *Org. Lett.* **2012**, *14*, 3660. (c) Tylleman, B.; Vande Velde, C. M. L.; Balandier, J.-Y.; Stas, S.; Sergeyev, S.; Geerts, Y. H. *Org. Lett.* **2011**, *13*, 5208.

(19) (a) Gorodetsky, A. A.; Chiu, C.-Y.; Schiros, T.; Palma, M.; Cox, M.; Jia, Z.; Sattler, W.; Kymissis, I.; Steigerwald, M.; Nuckolls, C. *Angew. Chem., Int. Ed.* **2010**, *49*, 7909. (b) Kang, S. J.; Kim, J. B.; Chiu, C.-Y.; Ahn, S.; Schiros, T.; Lee, S. S.; Yager, K. G.; Toney, M. F.; Loo, Y.-L.; Nuckolls, C. *Angew. Chem., Int. Ed.* **2012**, *51*, 8594.

(20) Laschat, S.; Baro, A.; Steinke, N.; Giesselmann, F.; Gele, C. H.; Scalia, G.; Judele, R.; Kapatsina, E.; Sauer, S.; Schreivogel, A.; Tosoni, M. *Angew. Chem., Int. Ed.* **2007**, *46*, 4832.

(21) (a) Zheng, H.; Lai, C. K.; Swager, T. M. *Chem. Mater.* **1995**, *7*, 2067. (b) Destrade, C.; Foucher, P.; Gesparoux, H.; Nguyen, H. T.; Levelut, A. M.; Malthete, J. *Mol. Cryst. Liq. Cryst.* **1984**, *106*, 121.

(22) The supplementary crystallographic data for this paper can be obtained free of charge from the Cambridge Crystallographic Data Centre via www.ccdc.cam.ac.uk/data_request/cif: (a) *syn*/*anti*-**1b** formed in *p*-xylene: CCDC-869826. (b) *syn*/*anti*-**1b** formed in toluene: CCDC-876942. (c) *syn*-**1b** formed in *p*-xylene: CCDC-895213.

(23) Liu, C.; Liu, Z.; Lemke, H. T.; Tsao, H. N.; Naber, R. C. G.; Li, Y.; Banger, K.; Müllen, K.; Nielsen, M. M.; Sirringhaus, H. *Chem. Mater.* **2010**, *22*, 2120.

(24) Zschieschang, U.; Ante, F.; Schlörholz, M.; Schmidt, M.; Kern, K.; Klauk, H. *Adv. Mater.* **2010**, *22*, 4489.

(25) Cornil, J.; Beljonne, D.; Calbert, J.-P.; Brédas, J.-L. *Adv. Mater.* **2001**, *13*, 1053.

(26) Pisula, W.; Tomovic, Z.; Simpson, C.; Kastler, M.; Pakula, T.; Müllen, K. *Chem. Mater.* **2005**, *17*, 4296.

(27) Balandier, J.-Y.; Quist, F.; Stas, S.; Tylleman, B.; Ragoen, C.; Mayence, A.; Bouzakraoui, S.; Cornil, J.; Geerts, Y. H. *Org. Lett.* **2011**, *13*, 548.

JACS
JOURNAL OF THE AMERICAN CHEMICAL SOCIETY

Communication

pubs.acs.org/JACS

Structurally Defined Graphene Nanoribbons with High Lateral Extension

Matthias Georg Schwab,[†,§] Akimitsu Narita,[†] Yenny Hernandez,[†,∥] Tatyana Balandina,[‡] Kunal S. Mali,[‡] Steven De Feyter,[‡] Xinliang Feng,[†] and Klaus Müllen*[,†]

[†]Max Planck Institute for Polymer Research, Ackermannweg 10, D-55128 Mainz, Germany

[‡]Division of Molecular and Nanomaterials, Department of Chemistry, and INPAC-Institute of Nanoscale Physics and Chemistry, Katholieke Universiteit Leuven, Celestijnenlaan, 200 F, B 3001 Leuven, Belgium

Supporting Information

ABSTRACT: Oxidative cyclodehydrogenation of laterally extended polyphenylene precursor allowed bottom-up synthesis of structurally defined graphene nanoribbons (GNRs) with unprecedented width. The efficiency of the cyclodehydrogenation was validated by means of MALDI-TOF MS, FT-IR, Raman, and UV–vis absorption spectroscopies as well as investigation of a representative model system. The produced GNRs demonstrated broad absorption extended to near-infrared region with the optical band gap of as low as 1.12 eV.

Graphene nanoribbons (GNRs), characterized by a large aspect ratio with lateral quantum confinement, are predicted to possess a band gap[1−5] in contrast to graphene which itself is a zero band gap semimetal.[6] It has been theoretically and experimentally demonstrated that both width and edge structure of GNRs strongly govern the electronic characteristics of graphene materials.[1,7,8] Their appealing electronic properties can only be accessed, however, if new methods for reliable and reproducible build-up of well-defined GNRs with precise lateral and longitudinal dimensions are developed. Top-down approaches such as lithographic "cutting" of graphene,[1,2] longitudinal "unzipping"[3] or "etching"[4] of carbon nanotubes, and the surfactant-assisted extraction from graphite dispersions[5] cannot reach the required chemical precision. In our search for synthetic pathways toward GNRs, we have worked out a bottom-up strategy that relies on the intramolecular oxidative cyclodehydrogenation[9,10] of tailored polyphenylene precursors.[11−15] Hence, a number of different GNR geometries have been realized, ranging from fully linear[11,14,15] to kinked.[12,13,15] The versatility of this method was successfully demonstrated both for solution-[11−14] and surface-based[15] protocols, resulting in GNRs of atomic accuracy. This stands in sharp contrast to the aforementioned top-down methods.[1−5]

GNRs so far fabricated by bottom-up approaches are limited to those with lateral dimensions smaller than 1 nm, which show absorption only up to 670 nm and calculated band gap larger than 1.6 eV.[11−15] For future applications in electronic devices, it is essential to synthesize GNRs with tailored band gaps. In this work, we present a solution synthesis and characterization of unprecedentedly broad, low band gap, and structurally defined GNRs, which can be derived from laterally extended polyphenylene precursors. For comparison, a representative model polycyclic aromatic hydrocarbon (PAH, **C78**,[16,17] with 78 carbon atoms in the aromatic core) of GNRs is also reported, for which a new efficient synthesis is validated by means of matrix-assisted laser desorption/ionization time-of-flight (MALDI-TOF) mass spectrometry (MS), ^{1}H NMR spectroscopy, and scanning tunneling microscope (STM).

First, *para*-terphenyl-based oligophenylene precursor **4a**, which corresponds to target PAH **C78**,[16,17] was designed as a model compound to examine its suitability for efficient cyclodehydrogenation (Scheme 1). Synthesis of **4a** was initiated with *Sonogashira-Hagihara* cross-coupling of 2,2″-diiodoterphenyl **1a** with trimethylsilyl acetylene followed by deprotection to yield 2,2″-diethynylterphenyl **2a**. Two-fold Diels–Alder cycloaddition between **2a** and functionalized tetraphenylcyclopentadienone **3**[18] under microwave conditions effi-

Scheme 1. Synthetic Route to PAH C78 and GNR 6[a]

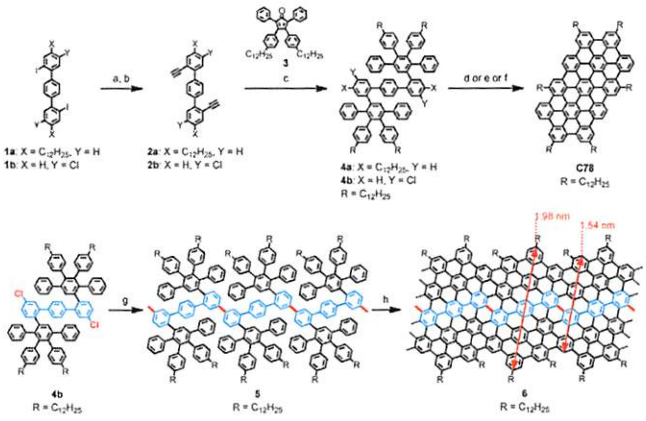

[a]Geometric dimensions of GNR **6** were derived from Merck Molecular Force Field 94 (MMFF94) calculations. Reagents and conditions: (a) trimethylsilyl acetylene, $Pd(PPh_3)_2Cl_2$/CuI, NEt_3, rt; (b) K_2CO_3, THF/MeOH, rt, **2a**: 51% (two steps), **2b**: 58% (two steps); (c) xylene, 160 °C, μW, 300 W, **4a**: 81%, **4b**: 85%; (d) $FeCl_3$, CH_2Cl_2/CH_3NO_2, rt, 93%; (e) $MoCl_5$, CH_2Cl_2, rt, 85%; (f) PIFA/BF_3, CH_2Cl_2, −60 °C, then −10 °C, 81%; (g) bis(cycloocta-(1,5)-diene)nickel(0) cycloocta-(1,5)-diene, 2,2′-bipyridine, toluene/DMF, 80 °C, 81%; (h) $FeCl_3$, CH_2Cl_2/CH_3NO_2, rt, 92%.

Received: August 3, 2012
Published: October 19, 2012

   dx.doi.org/10.1021/ja307697j | J. Am. Chem. Soc. 2012, 134, 18169−18172

ciently produced **4a** in 81% yield. Subsequent experiments confirmed that **4a** can be readily transformed into **C78** by using either the established $FeCl_3$ mediated cyclodehydrogenation[9,10,16,17] or less common oxidative procedures involving $MoCl_5$[10,19] or PIFA/BF_3.[10,18] In all three cases, characterization of the products by a combination of MALDI-TOF MS and ^{1}H NMR spectroscopy proved the formation of **C78** as an exclusive product (Figures 1 and S1). No partially fused

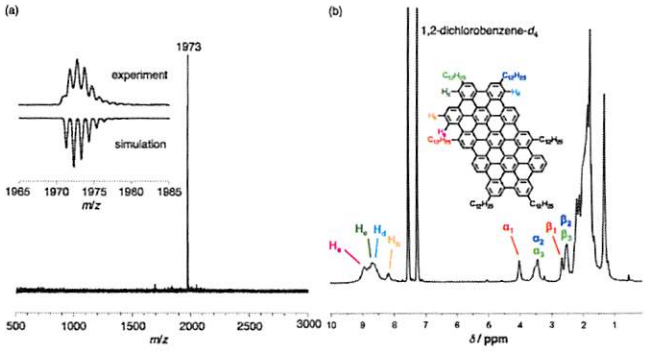

Figure 1. (a) MALDI-TOF MS spectrum of **C78**; inset: the isotopic distribution is in agreement with the simulated result. (b) ^{1}H NMR spectrum of **C78** in 1,2-dichlorobenzene-d_4 at 170 °C.

intermediates or chlorinated products could be detected by MALDI-TOF MS, and comparison of the isotropic distribution with simulation proved the complete cyclodehydrogenation (Figure 1a). Generally, PAHs suffer from strong aggregation in solution, which results in broadening of peaks in ^{1}H NMR spectroscopy.[20] Remarkably, however, a well resolved ^{1}H NMR spectrum could be recorded for **C78** at 170 °C by using high-boiling-point solvent, 1,2-dichlorobenzene-d_4 (Figure 1b). Because of its extended π-system, the signals of the protons on the aromatic backbone of **C78** appeared strongly downfield shifted in a range between δ = 8.0 and 9.5 ppm. With the help of peak integration and Nuclear *Overhauser* enhancement spectroscopy (NOESY) measurements, a number of aliphatic and aromatic signals could be assigned as indicated in Figure 1b, which further confirmed the chemical identity of the product. To our best knowledge, this is the largest PAH that allows for structural characterization by ^{1}H NMR.

Furthermore, STM rendered the visualization of **C78** at the solid–liquid interface of Au(111)/1,2,4-trichlorobenzene (TCB) (Figure 2a). The alkyl chains were surface-crystallized and split into a set of four lateral and two kinked longitudinal

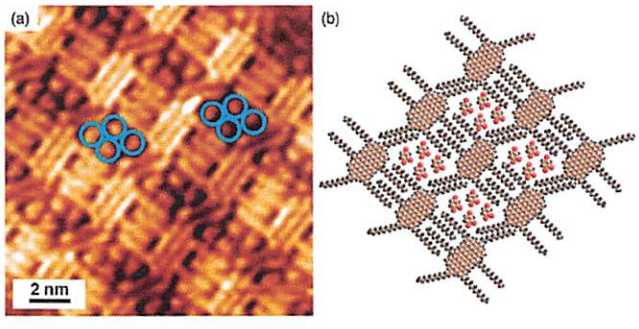

Figure 2. (a) STM image of **C78** physisorbed at the Au(111)/TCB interface; blue circles indicate entrapped guest molecules; imaging conditions: I_t = 0.1 nA, V_{bias} = 464 mV. (b) A tentative molecular model for the self-assembly of **C78** on Au (111).

chains. The aromatic core showed three parallel stripes running along the long axis, which correlated with electron densities in the highest occupied molecular orbitals.[17] The dimensions of the core extracted from the image (length = 2.3 ± 0.1 nm and width 1.4 ± 0.1 nm) were in good agreement with the values obtained by molecular modeling (Figure 2b). The remaining interspace between four **C78** molecules was filled with TCB guest molecules that appeared as small bright spots. These observations clearly support the defect-free synthesis of **C78** (see Supporting Information for more details). It should be mentioned here that, despite the successful synthesis of **C78** in previous reports,[16,17] the present protocol shows the obvious advantage regarding the cyclodehydrogenation efficiency of precursors that can avoid the rearrangement under the experimental conditions. More importantly, precursor **4** can be considered as a repeating unit of polyphenylene precursor **5** which renders one to produce laterally extended GNR **6** with a width of 1.54–1.98 nm (Scheme 1).

So far, all chemical routes toward the synthesis of polyphenylene precursors made use of A_2B_2-type polycondensation reactions such as *Suzuki-Miyaura* cross-coupling[11,12] and *Diels–Alder* reaction.[13,14] Because of the intrinsic sensitivity of these protocols to stoichiometry,[21] an *AA*-type *Yamamoto* polycondensation system which can circumvent this drawback is believed to be more efficient and can yield high molecular-weight precursors. Therefore, monomer **4b** substituted with reactive halogen groups was synthesized, allowing an *AA*-type Yamamoto polymerization to yield kinked polyphenylene precursor **5** (Scheme 1).[21] MALDI-TOF MS characterization of **5** indicated the presence of a regular pattern with molecular weight up to 35 000–40 000 g mol^{-1} (Figure 3a). On this basis,

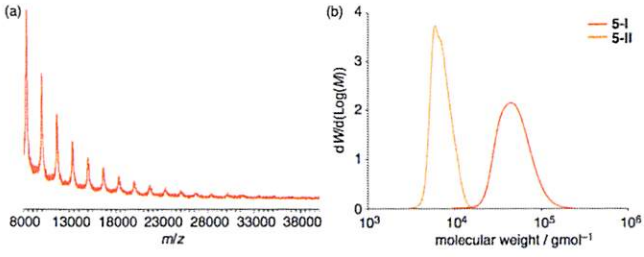

Figure 3. (a) Linear-mode MALDI-TOF MS spectra of polyphenylene precursor **5** (before separation). (b) Molecular weight distribution of **5-I** and **5-II** (SEC, eluent: THF, PS standard).

the number of repeating units in **5** was 21–24, which corresponded to approximately 30 nm of the resultant GNRs. This is most likely not the maximal value, however, due to the limitation of MALDI-TOF MS for the analysis of high-molecular-weight species with a broad molecular weight distribution.[12,22] Further investigation of **5** by size exclusion chromatography (SEC) revealed its relatively high polydispersity index (PDI) of 2.2. Therefore, the crude polymer **5** was separated into two fractions by utilizing preparative SEC. The fraction of larger molecular weight **5-I** showed weight-average molecular weight (M_w) of 52 000 g mol^{-1} with PDI of 1.2, whereas the other fraction of smaller molecular weight **5-II** showed M_w of 7200 g mol^{-1} with PDI of 1.1 (Figure 3b). These results based on SEC are approximately relative values according to the polystyrene (PS) standard calibration,[23] but they highlight the superiority of the *AA*-type Yamamoto approach over the A_2B_2-type polymerization for the preparation of high molecular weight precursors.[11–13]

dx.doi.org/10.1021/ja307697j | J. Am. Chem. Soc. 2012, 134, 18169–18172

Next, intramolecular cyclodehydrogenation of precursors **5**, **5-I**, and **5-II** was performed using $FeCl_3$ as oxidant in a mixture of dichloromethane and nitromethane, yielding GNRs **6**, **6-I**, and **6-II**, respectively. MALDI-TOF MS analysis of GNR **6-II** suggested a similar number of repeating units with respect to precursor **5-II** (Figure S11). However, GNRs **6** and **6-I** were precluded from MALDI-TOF MS characterization possibly owing to the strong aggregation of high molecular weight GNRs.[19,22]

Fourier transform infrared (FTIR) spectroscopy analysis of precursor **5** and GNR **6** showed the disappearance of the band at 4050 cm^{-1} which originates from the rotation of free phenyl rings (Figure 4).[13,24] Further, the signal triad at 3025, 3056, and

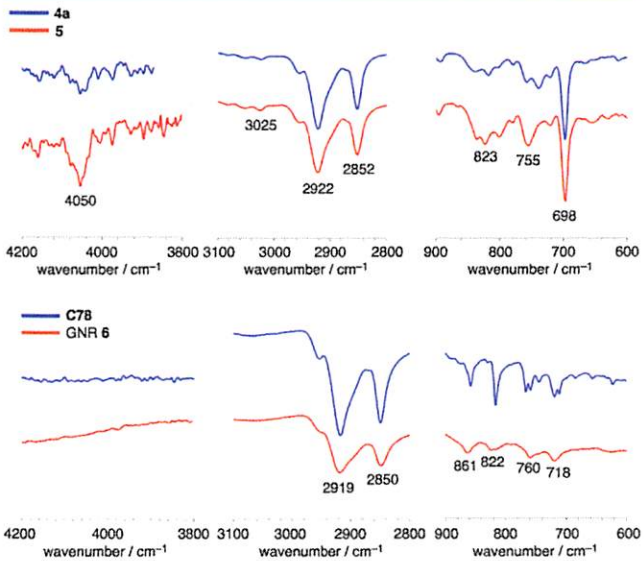

Figure 4. Representative FTIR spectral regions before (**4a**, **5**) and after (**C78**, GNR **6**) oxidative cyclodehydrogenation.

3083 cm^{-1} which is typical for aromatic C–H stretching vibrations was diminished, and the fingerprint bands at 698 and 755 cm^{-1} originating from monosubstituted benzene rings were attenuated.[24,25] These observations were in line with the analogous conversion of model compound **4a** into **C78**, and indicated highly efficient "graphitization" of precursor **5** into GNR **6**. Raman spectrum of a powder sample of GNR **6-I** was measured at 488 nm with laser power of 1 mW, and showed first-order D band (disorder band) and G band (graphite band) at 1316 and 1595 cm^{-1}, respectively, consistent with literature values for GNRs (Figure 5a).[3,4,15,26] The relatively high intensity of the D band could be explained by the contribution of the edges as defects.[4,12,15,26] Moreover, well-resolved double-resonant signals were also observed at 2632, 2910, and 3194 cm^{-1}, which could be assigned to 2D, D+G, and 2G bands, respectively.[26] It should be mentioned that the G* band (~2450 cm^{-1}) typical for graphene was apparently too small to be observed, because a powder (multilayer) sample was used for the measurement in this work.[26d]

The GNR samples were virtually insoluble in conventional organic solvents such as dichloromethane, chloroform, and toluene. However, use of *N*-methylpyrrolidone (NMP), which is known as a good solvent for the exfoliation of graphene[27] as well as for the debundling of carbon nanotubes,[28] enabled the exfoliation of GNRs with the assistance of mild sonication to obtain stable dispersions (~60 μg/mL) (Figure 5b, inset).

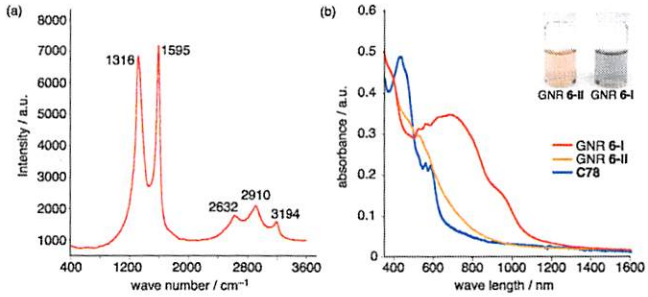

Figure 5. (a) Raman spectrum of GNR **6-I** measured at 488 nm (powder, laser power: 1 mW). (b) Normalized UV–vis absorption spectra of GNR **6-I** (red, in NMP), GNR **6-II** (orange, in NMP), and **C78** (blue, in THF); inset: a picture of solutions of GNR **6-I** and **6-II** in NMP.

Thus, UV–vis absorption spectra of GNR **6-I** and **6-II** were recorded in NMP and compared with that of **C78** (17 μM in THF) as shown in Figure 5b. For **C78**, the β-band was observed at 431 nm and the p- and α-band were located at 514 and 580 nm, respectively. The relatively high intensity of the α-band could be attributed to the low symmetry of **C78**.[18,29] The optical band gap of **C78** could not be determined from the onset of the p-band due to the broadened absorption bands,[29] but was estimated to be larger than 1.92 eV from the absorption edge of 647 nm. It is remarkable to note that the longest GNR **6-I** showed absorption peaks at 690 and 960 nm with broad absorption extended to the near-infrared (NIR) region. The absorption edges of GNR **6-I** and **6-II** were derived from the spectra to be 1109 and 812 nm, corresponding to the optical band gap of 1.12 and 1.53 eV, respectively. Thereby, this result undoubtedly demonstrated the extraordinarily low band gap of the laterally extended GNRs compared to previously bottom-up synthesized GNRs.[11–15] Furthermore, the optical band gap of 1.12 eV is in a good agreement with the calculated band gap of 1.08 eV, proving that GNR **6-I** is sufficiently elongated, namely more than 15 repeating units, or approximately 20 nm, to obtain the lowest band gap achievable with its lateral structure.[30]

In summary, structurally defined and laterally extended GNRs were synthesized via a bottom-up chemical approach. Characterizations by MALDI-TOF MS, FTIR, Raman, and UV–vis absorption spectroscopies as well as investigation of a model system validated the efficiency of the cyclodehydrogenation. For the first time, it was possible to access GNRs with band gap as low as 1.12 eV, reaching a broad absorption up to the NIR region. These GNRs may hold the potential in a number of opoelectronic devices such as solar cell, optical switching, and infrared imaging.

■ ASSOCIATED CONTENT

Supporting Information

Experimental details, NMR, MALDI-TOF MS, UV–vis absorption, fluorescence, and DSC spectra. This material is available free of charge via the Internet at http://pubs.acs.org.

■ AUTHOR INFORMATION

Corresponding Author

muellen@mpip-mainz.mpg.de

Present Addresses

[§]BASF SE, Carl-Bosch-Strasse 38, 67056 Ludwigshafen, Germany

[||]Physics Department, Universidad de los Andes, Carrera 1 18A-10, Bloque Ip. Bogotá, Colombia

Notes

The authors declare no competing financial interest.

■ ACKNOWLEDGMENTS

We are grateful to the financial support from ERC grant on NANOGRAPH, EU Project SUPERIOR (PITN-GA-2009-238177) and GENIUS, DFG Priority Program SPP 1459, ESF Project GOSPEL (Ref Nr: 09-EuroGRAPHENE-FP-001), the Max Plank Society through the program ENERCHEM, DFG Priority Program SPP 1355, DFG MU 334/32-1.

■ REFERENCES

(1) Han, M. Y.; Özyilmaz, B.; Zhang, Y.; Kim, P. *Phys. Rev. Lett.* **2007**, *98*, 206805.

(2) (a) Özyilmaz, B.; Jarillo-Herrero, P.; Efetov, D.; Kim, P. *Appl. Phys. Lett.* **2007**, *91*, 192107. (b) Jia, X.; Hofmann, M.; Meunier, V.; Sumpter, B. G.; Campos-Delgado, J.; Romo-Herrera, J. M.; Son, H.; Hsieh, Y. P.; Reina, A.; Kong, J. *Science* **2009**, *323*, 1701.

(3) (a) Kosynkin, D. V.; Higginbotham, A. L.; Sinitskii, A.; Lomeda, J. R.; Dimiev, A.; Price, B. K.; Tour, J. M. *Nature* **2009**, *458*, 872. (b) Shimizu, T.; Haruyama, J.; Marcano, D. C.; Kosinkin, D. V.; Tour, J. M.; Hirose, K.; Suenaga, K. *Nat. Nanotechnol.* **2011**, *6*, 45.

(4) Jiao, L.; Zhang, L.; Wang, X.; Diankov, G.; Dai, H. *Nature* **2009**, *458*, 877.

(5) Li, X.; Wang, X.; Zhang, L.; Lee, S.; Dai, H. *Science* **2008**, *319*, 1229.

(6) (a) Wallace, P. R. *Phys. Rev. Lett.* **1947**, *71*, 622. (b) Castro Neto, A. H.; Guinea, F.; Peres, N. M. R.; Novoselov, K. S.; Geim, A. K. *Rev. Mod. Phys.* **2009**, *81*, 109.

(7) (a) Schwierz, F. *Nat. Nanotechnol.* **2010**, *5*, 487. (b) Chen, Z.; Lin, Y. M.; Rooks, M. J.; Avouris, P. *Physica E* **2007**, *40*, 228.

(8) (a) Barone, V.; Hod, O.; Scuseria, G. E. *Nano Lett.* **2006**, *6*, 2748. (b) Yang, L.; Park, C.-H.; Son, Y.-W.; Cohen, M. L.; Louie, S. G. *Phys. Rev. Lett.* **2007**, *99*, 186801. (c) Radovic, L. R.; Bockrath, B. *J. Am. Chem. Soc.* **2005**, *127*, 5917.

(9) Scholl, R.; Seer, C. *Liebigs Ann. Chem.* **1912**, *394*, 111.

(10) Rempala, P.; Kroulík, J.; King, B. T. *J. Am. Chem. Soc.* **2004**, *126*, 15002.

(11) Yang, X.; Dou, X.; Rouhanipour, A.; Zhi, L.; Räder, H. J.; Müllen, K. *J. Am. Chem. Soc.* **2008**, *130*, 4216.

(12) Dössel, L.; Gherghel, L.; Feng, X.; Müllen, K. *Angew. Chem., Int. Ed.* **2011**, *50*, 2540.

(13) Wu, J.; Gherghel, L.; Watson, M. D.; Li, J.; Wang, Z.; Simpson, C. D.; Kolb, U.; Müllen, K. *Macromolecules* **2003**, *36*, 7082.

(14) Fogel, Y.; Zhi, L.; Rouhanipour, A.; Andrienko, D.; Räder, H. J.; Müllen, K. *Macromolecules* **2009**, *42*, 6878.

(15) Cai, J.; Ruffieux, P.; Jaafar, R.; Bieri, M.; Braun, T.; Blankenburg, S.; Muoth, M.; Seitsonen, A. P.; Saleh, M.; Feng, X.; Müllen, K.; Fasel, R. *Nature* **2010**, *466*, 470.

(16) (a) Müller, M.; Iyer, V. S.; Kübel, C.; Enkelmann, V.; Müllen, K. *Angew. Chem., Int. Ed.* **1997**, *36*, 1607. (b) Morgenroth, F.; Kübel, C.; Müller, M.; Wiesler, U. M.; Berresheim, A. J.; Wagner, M.; Müllen, K. *Carbon* **1998**, *36*, 833.

(17) Böhme, T.; Simpson, C.; Müllen, K.; Rabe, J. *Chem.—Eur. J.* **2007**, *13*, 7349.

(18) Takada, T.; Arisawa, M.; Gyoten, M.; Hamada, R.; Tohma, H.; Kita, Y. *J. Org. Chem.* **1998**, *63*, 7698.

(19) Kramer, B.; Fröhlich, R.; Waldvogel, S. *Eur. J. Org. Chem.* **2003**, 3549.

(20) (a) Wasserfallen, D.; Kastler, M.; Pisula, W.; Hofer, W. A.; Fogel, Y.; Wang, Z.; Müllen, K. *J. Am. Chem. Soc.* **2006**, *128*, 1334. (b) Kastler, M.; Pisula, W.; Wasserfallen, D.; Pakula, T.; Müllen, K. *J. Am. Chem. Soc.* **2005**, *127*, 4286.

(21) (a) Carothers, W. H. *Trans. Faraday Soc.* **1936**, *32*, 39. (b) Odian, G. G. *Principles of Polymerization*; J. Wiley & Sons: Hoboken, NJ, 2004.

(22) Martin, K.; Spickermann, J.; Räder, H. J.; Müllen, K. *Rapid Commun. Mass Spectrom.* **1996**, *10*, 1471.

(23) The PS standard was used for the SEC analysis instead of the poly(*para*-phenylene) standard, considering the kinked and nonrigid structure of polyphenylene precursor **5**.

(24) Centrone, A.; Brambilla, L.; Renouard, T.; Gherghel, L.; Mathis, C.; Müllen, K.; Zerbi, G. *Carbon* **2005**, *43*, 1593.

(25) Shifrina, Z. B.; Averina, M. S.; Rusanov, A. L.; Wagner, M.; Müllen, K. *Macromolecules* **2000**, *33*, 3525.

(26) (a) Malard, L. M.; Pimenta, M. A.; Dresselhaus, G.; Dresselhaus, M. S. *Phys. Rep* **2009**, *473*, 51. (b) Ryu, S.; Maultzsch, J.; Han, M. Y.; Kim, P.; Brus, L. E. *ACS Nano* **2011**, *5*, 4123. (c) Bischoff, D.; Güttinger; Dröscher, S.; Ihn, T.; Ensslin, K.; Stampfer, C. *J. Appl. Phys.* **2011**, *109*, 073710. (d) Yoon, D.; Moon, H.; Cheong, H.; Choi, J. S.; Choi, J. A.; Park, B. H. *J. Korean Phys. Soc.* **2009**, *55*, 1299.

(27) Hernandez, Y.; Nicolosi, V.; Lotya, M.; Blighe, F. M.; Sun, Z.; De, S.; McGovern, I. T.; Holland, B.; Byrne, M.; Gun'Ko, Y. K.; Boland, J. J.; Niraj, P.; Duesberg, G.; Krishnamurthy, S.; Goodhue, R.; Hutchison, J.; Scardaci, V.; Ferrari, A. C.; Coleman, J. N. *Nat. Nanotechnol* **2008**, *3*, 563.

(28) Bergin, S. D.; Nicolosi, V.; Streich, P. V.; Giordani, S.; Sun, Z.; Windle, A. H.; Ryan, P.; Niraj, N. P. P.; Wang, Z.-T. T.; Carpenter, L.; Blau, W. J.; Boland, J. J.; Hamilton, J. P.; Coleman, J. N. *Adv. Mater.* **2008**, *20*, 1876.

(29) Rieger, R.; Müllen, K. *J. Phys. Org. Chem.* **2010**, *23*, 315.

(30) Osella, S.; Narita, A.; Schwab, M. G.; Hernandez, Y.; Feng, X.; Müllen, K.; Beljonne, D. *ACS Nano* **2012**, *6*, 5539.